



Experimental Study on Fracture Propagation of Tight Sandstone Under the True Triaxial Fracturing with Supercritical CO₂

Zhi-fan Yang^{1,2}✉, Wen-zhe Li¹, Jun-liang Peng^{1,2}, Huan Peng^{1,2}, and Yun-tao Liu^{1,2}

¹ Engineering Technology Research Institute of Southwest Oil and Gas Field Company, PetroChina, Chengdu, China
805873240@qq.com

² Key Laboratory Reservoir Stimulation, CNPC, Chengdu, China

Abstract. Supercritical CO₂ fracturing is a novel fracturing technology that boasts significant benefits, including the reduction of reservoir pollution and the achievement of thorough backflow following the fracturing process. Guided by the “dual carbon” goal, supercritical CO₂ fracturing technology has broad application prospects. Due to the limited research on the fracture propagation law of tight sandstone in the Sichuan Basin by supercritical CO₂, it cannot effectively guide the development of supercritical CO₂ fracturing plans. Based on the true triaxial fracturing simulation experimental system, experimental research on supercritical CO₂ fracturing of tight sandstone was conducted to study how fracturing fluid type, displacement, and horizontal stress difference affect the fracture propagation law. The research shows that: First, the fracture pressure of supercritical CO₂ is 9.5 MPa lower than that of slick water, with an average decrease of 40.6%, and the rock fracture time increases by 274.1%. The fracture tortuosity and fracture surface roughness are larger, and the fracture network is more complex, which can provide more effective percolation channels for the formation fluids. Second When the injection rate of supercritical CO₂ increases from 30 mL/min to 60 mL/min, the fracture pressure increases by 26.5%, the fracture time decreases by 43.3%, the number of branch fractures increases, and the angle between branch fractures and main fractures increases. Third, When the horizontal stress difference increases from 6 MPa to 10 MPa, the fracture pressure increases by 31.4%, and the fracture

Copyright 2023, IFEDC Organizing Committee.

This paper was prepared for presentation at the 2023 International Field Exploration and Development Conference in Wuhan, China, 20–22 September 2023.

This paper was selected for presentation by the IFEDC Committee following review of information contained in an abstract submitted by the author(s). Contents of the paper, as presented, have not been reviewed by the IFEDC Technical Team and are subject to correction by the author(s). The material does not necessarily reflect any position of the IFEDC Technical Committee its members. Papers presented at the Conference are subject to publication review by Professional Team of IFEDC Technical Committee. Electronic reproduction, distribution, or storage of any part of this paper for commercial purposes without the written consent of IFEDC Organizing Committee is prohibited. Permission to reproduce in print is restricted to an abstract of not more than 300 words; illustrations may not be copied. The abstract must contain conspicuous acknowledgment of IFEDC. Contact email: paper@ifedc.org.

time decreases by 7.5%. The fracturing fracture (HF) mainly extends along the direction of the maximum horizontal principal stress, which is not conducive to multi-point fracture initiation and fracture turning. This study clarified the influence of different fluids, displacement, and stress differences on the propagation of tight sandstone fractures through a large-scale true triaxial fracturing experimental device, providing a strong theoretical basis and experimental support for CO₂ fracturing and on-site CO₂ storage in tight sandstone gas reservoirs.

Keywords: Tight sandstone · Supercritical CO₂ · True triaxial fracturing · CT scanner

1 Introduction

Supercritical CO₂ has gained significant attention over recent years as a novel form of fracturing fluid. This is attributed to its advantageous properties, including high density, low viscosity, high diffusion coefficient, low surface tension, and superb heat and mass transfer performance [1–3]. For tight sandstone reservoirs, experimental research on fracture propagation through supercritical CO₂ fracturing has found that The commencement force for fracturing using supercritical CO₂ is approximately 28.2% less than that of utilizing slick water. Furthermore, there is an increased complexity of fractures in conditions with low horizontal stress differences [4–6]. Supercritical CO₂ does not cause damage to the reservoir and is prone to backflow, effectively avoiding near wellbore formation blockage, protecting oil and gas reservoirs, and improving reservoir permeability [7, 8]. In tight sandstone, CO₂ generates calcite precipitation through physical and chemical interaction with reservoir minerals, which can also realize the local storage of CO₂, thus reducing environmental pressure [9, 10]. Therefore, supercritical CO₂ has the potential for reservoir transformation, carbon utilization, and carbon sequestration. Guided by the “dual carbon” goal, the technology of fracturing using supercritical CO₂ exhibits vast potential for application in various fields.

With the proposal and development of supercritical CO₂ fracturing technology, the study of fracture propagation law in such technology is a crucial aspect. Zhang X et al. [11] used CT scanning technology to compare fracture propagation in water, liquid CO₂ and supercritical CO₂, and reflected changes in fracture pressure through AE signals; JIANG Y [12] plotted injection pressure and temperature curves and proposed the mechanism of expansion and thermal stress promoting fracture propagation using active acoustic waves P and S waves. Zhou D [13, 14] conducted visualization experiments on fracture propagation in supercritical CO₂ and believed that CO₂ phase transition leads to dynamic fracture propagation and the formation of complex fractures. Chen H [15] used cement specimens to test the influence of supercritical CO₂ on the complexity of fractures, and believed that the stress state has a significant impact on supercritical CO₂ fracturing. Due to the lack of systematic research on the initiation and fracturing of tight sandstone in the Sichuan Basin, fracture propagation patterns, and post fracturing fracture morphology caused by supercritical CO₂ and slickwater, it is not possible to effectively guide the formulation of supercritical CO₂ fracturing plans. In combination with the geological characteristics and engineering needs of the block, this paper uses

the Shaximiao formation outcrop in Sichuan Basin and uses a large true triaxial fracturing experimental device and CT scanner to carry out true triaxial supercritical CO₂ and slick water fracturing experimental study in tight sandstone, and focus on quantifying the fracture pressure, tortuosity and fractal dimension of fractures in tight sandstone in Sichuan Basin while investigating the impact of various fluids, flow rates, and stress disparities on tight sandstone fracture expansion. This study aims to address the significant challenges associated with supercritical CO₂ fracturing in tight sandstone.

2 Experimental Apparatus

The experimental apparatus employed for the true triaxial fracturing experiment consists of several components, including a triaxial model system, confining pressure system, heating control system, preheating system, pumping system, measurement system, and data acquisition system. The procedure for the experiment is illustrated in Fig. 1. To simulate hydraulic fracturing, similarity criteria were followed [16, 17]. Samples with lower strength were used or the viscosity of the fracturing fluid was increased to reduce the impact of fracture toughness on fracture growth, avoid dynamic fracture growth during the fracturing experiment and affect the experimental results.

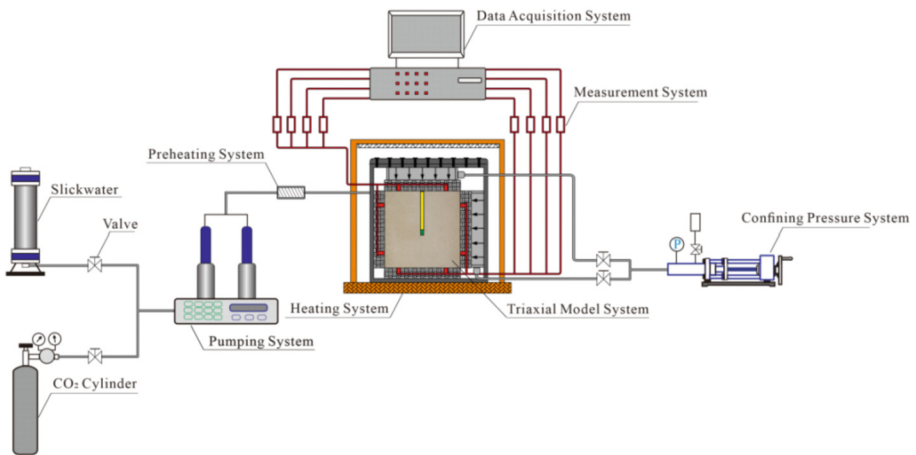


Fig. 1. Flow Chart of True Triaxial Fracturing Experimental Device.

CT scanners measure the object being measured by emitting an X-ray beam, and then establish a 3D image of the object based on the differences in X-ray absorption and transmittance of different components within the object using a computer processing system. The CT scanning system allows for real-time observation and imaging of the internal structure evolution of the specimen during the experimental process, accurately reflecting the internal structure of rock bedding, fractures, and other structures. It is a completely non-destructive testing technology for rock samples.

In order to get the coordinate parameters of the fracture surface and further analyze the parameters such as tortuosity and roughness of the fracture surface [18], some rock

specimens after fracturing were cut open and Trimble FX 3D laser scanner was used. Scan the fracture surface of the rock specimen to obtain the scanning data point coordinates x , y , and z , and the data collection is based on the laser triangle principle.

3 Experimental Samples and Methods

To guarantee the selected rock samples' representativeness, a systematic field survey was performed on the Shaximiao Formation outcrop in the Sichuan Basin. The survey aimed to identify the reservoir's outcrop location, followed by a comparison of the mineral composition, microstructure, and other characteristics of the outcrop and formation core. Finally, the Shaximiao Formation tight sandstone outcrop samples in the Jiangyou area, Mianyang, Sichuan were selected. After retrieving the samples from the field to the indoor area, the sandstone was processed into a cube specimen with a side length of 20 cm, and a simulated wellbore with a diameter of 1.2 cm and a height of 11 cm was drilled in the middle of the specimen. Special chemical adhesive (AB adhesive) is used to fix the steel injection pipe into the simulated wellbore of the specimen, which is used to simulate the fracturing wellbore. To obtain the required samples for the true triaxial physical simulation experiment, we have designed the injection pipe with a sealing length of 9 cm, which includes a 2 cm open hole section located at the center of the specimen. Our laboratory study focuses on the true triaxial supercritical CO₂ and slick water fracturing of tight sandstone. This study aims to investigate the impact of various factors such as different fluids, displacement, and stress differences on the propagation of tight sandstone fractures. To conduct the experiments, we have developed a specific experimental plan detailed in Table 1, and the experimental temperature has been set at 40 °C.

Table 1. Functional parameters of the proppant transport characteristic complex fracture experimental device.

Sample no.	Rock type	Fluid	Injection Displacement (mL/min)	Triaxial Stress ($\sigma_V/\sigma_H/\sigma_h$) MPa
1	Sandstone	slickwater	30	8/12/4
2	Sandstone	supercritical CO ₂	30	8/12/4
3	Sandstone	supercritical CO ₂	40	8/12/4
4	Sandstone	supercritical CO ₂	60	8/12/4
5	Sandstone	supercritical CO ₂	30	8/10/4
6	Sandstone	supercritical CO ₂	30	8/14/4

Among them, in order to simulate the crustal stress state of vertical wells in tight sandstone reservoirs [19, 20], triaxial hydraulic loading is used to achieve triaxial stress loading, and the minimum horizontal principal stress is applied respectively σ_H and

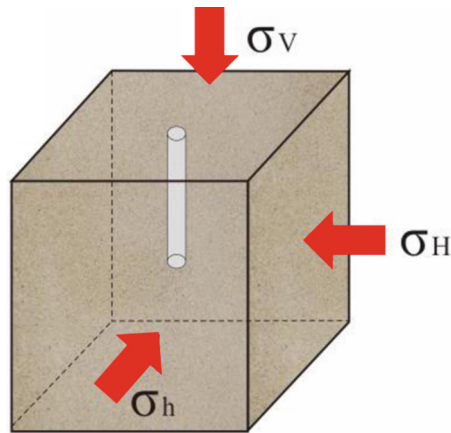


Fig. 2. Schematic diagram of stress loading on a true triaxial large physical model.

maximum horizontal principal stress σ_H perpendicular to the wellbore axis, vertical stress σ_V is parallel to the wellbore axis, as shown in Fig. 2.

Based on the experiment's objectives and plan, the procedure for conducting the experiment entails the following steps:

- (1) To clarify the internal bedding and natural fracture distribution of tight sandstone, CT scans were performed on the prepared samples;
- (2) Seal the test piece into the rubber sleeve and let it air dry for 3 days. After checking the sealing of the equipment, place the test piece into the loading triaxial pressure chamber;
- (3) Connect the fracturing fluid injection pump, injection pipeline, and simulated wellbore;
- (4) After inspecting the entire pipeline and data collection system, according to the experimental conditions in Table 1, preheat the loading chamber in a water bath for 30 min to subject the sample to three-dimensional stress loading;
- (5) Turn on the heater for heating, start the booster pump and data acquisition software, inject fluid, and start the fracturing experiment;
- (6) After the fracturing experiment is completed, stop the booster pump and data acquisition software, and slowly unload the three-dimensional stress to normal pressure;
- (7) Remove the loading device from the water bath, retrieve the sample, take photos and record, use CT to scan the fracturing sample, and take photos to record the fracture morphology.

4 Experimental Results and Analysis

4.1 The Influence of Fluid Type on the Propagation Law of Fractures in Tight Sandstone

In terms of fracture pressure, due to the small size of the sample, when the ultimate strength is reached around the wellbore, the initiation and propagation of fractures occur almost simultaneously, so the peak value of the curve is considered as the initiation pressure. The fracturing curve of supercritical CO₂ and slick water fracturing is shown in Fig. 3.

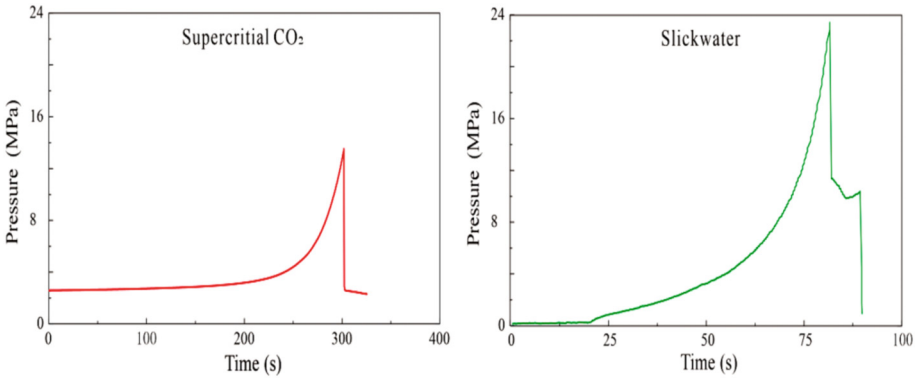


Fig. 3. Fracturing curve of supercritical CO₂ and slickwater.

From the figure, it illustrates that under the conditions of a stress difference of 8MPa and a displacement of 30 mL/min, the fracture pressure of supercritical CO₂ is 13.9 MPa, rock fracture takes 303 s, the fracture pressure of slickwater is 23.4 MPa, rock fracture takes 81 s. This indicates that compared to slickwater, the fracture pressure of supercritical CO₂ has been observed to decline by 9.5 MPa, with a mean reduction of 40.6%, and the rock fracture time has increased by 274.1%. This is because the surface tension of supercritical CO₂ is extremely low, so supercritical CO₂ fracturing only requires a small amount of internal pressure to extend, while smooth water has a higher surface tension and can only enter large-scale fractures. The pressure-acting distance inside the fractures is short, which is not conducive to activating micro fractures and leading to fracture pressure. The pressure change curve of sandstone during supercritical CO₂ fracturing can be clearly categorized into three distinct stages: compression stage, rapid pressurization stage, and fracture initiation and failure stage. In the compression stage, the initial CO₂ quickly fills the pipeline and holes, and the high compression characteristics of supercritical CO₂ make it exhibit a gentle pressurization phenomenon, and enter the rapid pressurization stage. The pressure curve shows a sharp rise, showing a linear growth similar to the water fracturing curve. The pressure change curve of smooth hydraulic fracturing sandstone during the initial injection stage is slow due to the discharge of air from the pipeline and borehole. Once filled, the pressure within the specimen increases

rapidly, leading to its eventual damage and a subsequent notable extension of the time taken for rock fracture.

In terms of fracture morphology, the fracture morphology formed by supercritical CO_2 and slick water fracturing under the same injection displacement and stress difference conditions is shown in Fig. 4.

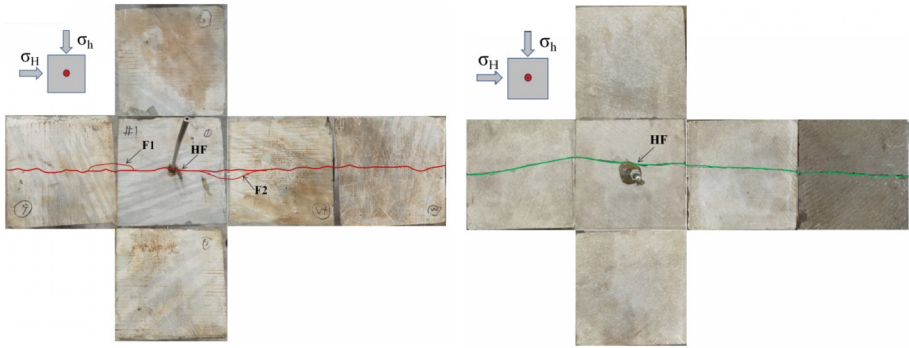


Fig. 4. Fracture morphology diagram of supercritical CO_2 (left) and slick water (right) fracturing.

From the figure, it illustrates that the hydraulic fracture HF formed by supercritical CO_2 fracturing extends along the direction of the maximum horizontal principal stress. During the fracture process, it is common for branch fractures, such as F1 and F2, to form and slightly deviate from their original propagation direction. This leads to the creation of an intricate network of fractures where the major and minor fractures intersect and connect with each other. The hydraulic fracture HF formed by smooth water fracturing starts at the open hole section and extends along the direction of the maximum horizontal principal stress to form a simple transverse fracture with a relatively straight and single fracture morphology.

As the main seepage channel in the sandstone after reservoir reconstruction, the artificial fracturing fracture directly determines the quality of the fracturing effect. The fracture characteristics mainly include: fracture space morphology, complexity, tortuosity and roughness of the fracture surface and other parameters. To further study the fracture morphology after fracturing with different fluids, CT scans were performed on the rock core to obtain the distribution and type of fracturing fractures, as shown in Fig. 5.

The figure reveals that supercritical CO_2 fracturing yields a more intricate and uneven fracture surface in contrast to hydraulic fracturing. Tortuosity, the proportion of the actual fracture length to the straight-line length, reflects the fluid flow's curvature within the fracture. To determine fractal tortuosity, the rock specimen's fracture surface underwent 3D laser scanning. The resulting data indicates that the tortuosity of supercritical CO_2 fracturing is 2.23 times higher than that of hydraulic fracturing. The surface roughness of the fracture is larger and the spatial morphology of the fracture is more complex, which helps to provide a more effective seepage channel for the formation fluid.

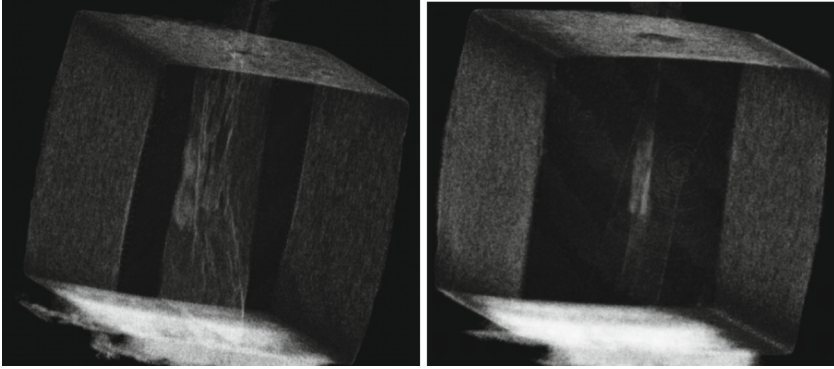


Fig. 5. CT scan images of supercritical CO₂ (left) and slick water (right) after fracturing.

4.2 The Influence of Injection Displacement Rate on the Fracture Propagation Law in Tight Sandstone

The injection displacement rate is another important engineering factor that affects the morphology of hydraulic fractures. To study the effect of different injection rates on fracture pressure and fracture propagation, the fracture curves of supercritical CO₂ under different injection rates under the condition of 8 MPa horizontal stress difference are shown in Fig. 6.

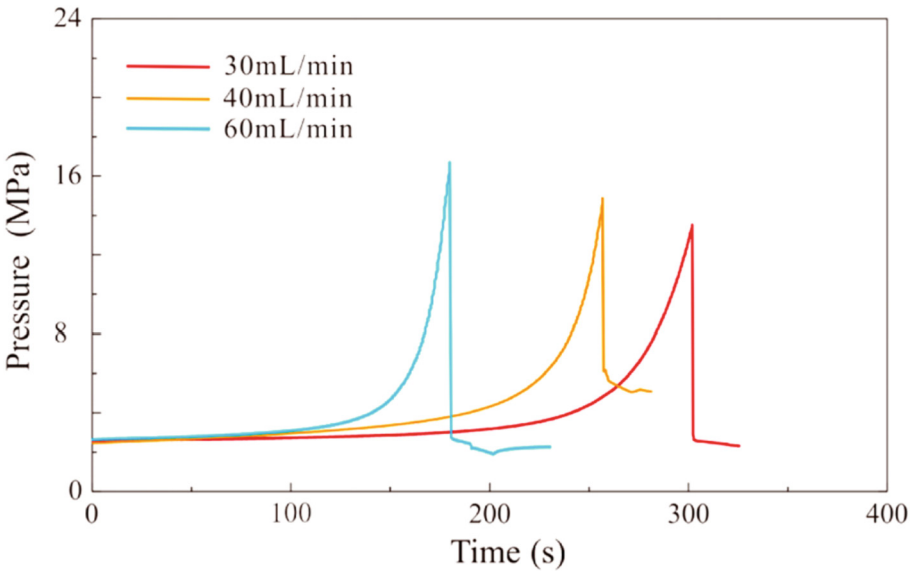


Fig. 6. Fracturing curves of supercritical CO₂ at different injection rates

From the figure, it illustrates that given similar horizontal stress differential conditions, an increase in supercritical CO₂ displacement from 30 mL/min to 40 mL/min

caused a 11.1% rise in fracture pressure from 13.6 MPa to 15.1 MPa, while the fracture time declined by 13.3% from 300 s to 260 s. However, when the displacement was further increased to 60 mL/min, the fracture pressure rose by 26.5% to 17.2 MPa, and the fracture time decreased by 43.3% to 170 s. It should be noted that an increase in injection displacement results in a more rapid CO₂ pressurization rate during the pore pressurization phase, which reduces the time required to inject the identical volume of CO₂. Owing to the restricted permeability of the tight sandstone matrix, the infiltration rate of CO₂ into the pores of the matrix shows no significant enhancement. Consequently, an elevated injection displacement causes an increment in initiation pressure and a reduction in fracture time.

In terms of fracture morphology, under the condition of 8 MPa horizontal stress difference, the fracture morphology of supercritical CO₂ under different injection displacement rates is shown in Fig. 7.

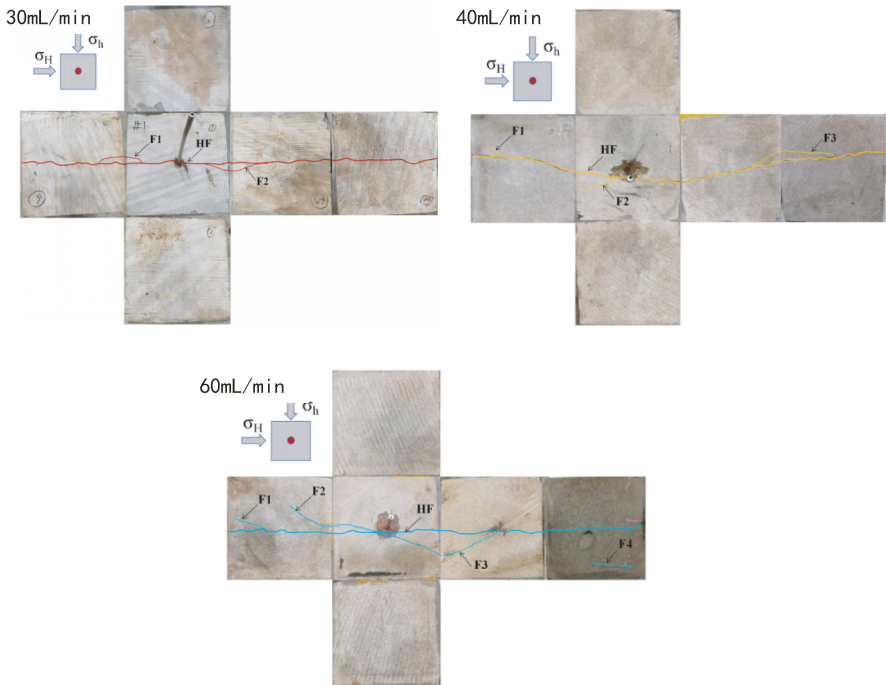


Fig. 7. Fracture morphology diagram of supercritical CO₂ fracturing under different injection rates

From the figure, it illustrates that under the 8 MPa horizontal stress difference, the hydraulic fracture HF formed by supercritical CO₂ fracturing extends along the direction of the maximum horizontal principal stress at an injection flow rate of 30 mL/min. Furthermore, branching fractures F1 and F2 are produced. At 40 mL/min, the hydraulic fracture HF extends along the direction of the maximum horizontal principal stress angle of 6.8°, generating additional branching fractures F1, F2, and F3. Finally, at 60 mL/min,

supercritical CO₂ fracturing forms the hydraulic fracture HF, which extends along the direction of the maximum horizontal principal stress while creating branch fractures F1, F2, F3, and F4. The angle between the branch crack and the main crack is 13–24°. Overall, as the displacement increases, the number of branch fractures grows, and the angle between the branch fractures and the main fracture increases. Additionally, the length of the branch fractures will increase, leading to the formation of a complex fracture network where the main and branch fractures communicate with each other. This is due to the increase of CO₂ discharge, the continuous accumulation of energy in the fracture, the increase of pore pressure gradient, and the accumulation of Strain energy stress, which lead to the increase of normal and tangential flow velocity in the fracture, the obvious increase of pressure, the shortening of fracture initiation time, the shortening of fracture propagation time, and the increasing of propagation speed.

4.3 The Influence of Horizontal Stress Difference on the Fracture Propagation Law in Tight Sandstone

The horizontal stress difference is an important geological factor that determines the propagation form of hydraulic fractures. To study the effect of different stress differences on fracture pressure and fracture propagation law, the fracture curves of supercritical CO₂ under different stress differences at a displacement of 30 mL/min are shown in Fig. 8.

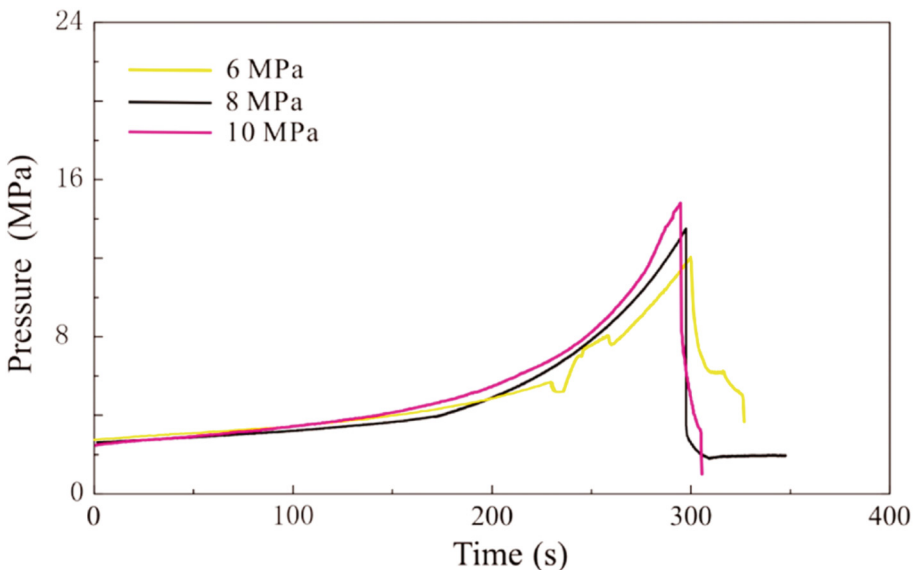


Fig. 8. Fracturing curves of supercritical CO₂ under different stress differences.

From the figure, it illustrates that at a displacement rate of 30 mL/min, the fracture pressure and fracture time differ when the horizontal stress variation changes. With a

horizontal stress difference of 6 MPa, rock fracture pressure is 11.8 MPa, and the fracture time is 305 s. However, the horizontal stress difference is 8 MPa, rock fracture pressure is 13.6 MPa, and the fracture time is 300 s. This represents a coefficient increase of 15.3% in fracture pressure and a decrease of 1.6% in fracture time. At a higher horizontal stress difference of 10 MPa, the fracture pressure and fracture time are 15.5 MPa and 282 s, respectively, signifying a 31.4% increase in fracture pressure and a 7.5% decrease in fracture time. The hydraulic fracture is influenced by internal pressure, in-situ stress, and other factors leading to increased pressure required for fracture initiation when the horizontal stress difference is large. As the fracture extends a certain distance, the hydraulic fracture experiences reduced resistance when subjected to horizontal traction, primarily towards the direction of maximum horizontal principal stress, resulting in decreased expansion pressure.

In terms of fracture morphology, the fracture morphology of supercritical CO₂ under different stress differences at a displacement of 30 mL/min is shown in Fig. 9.

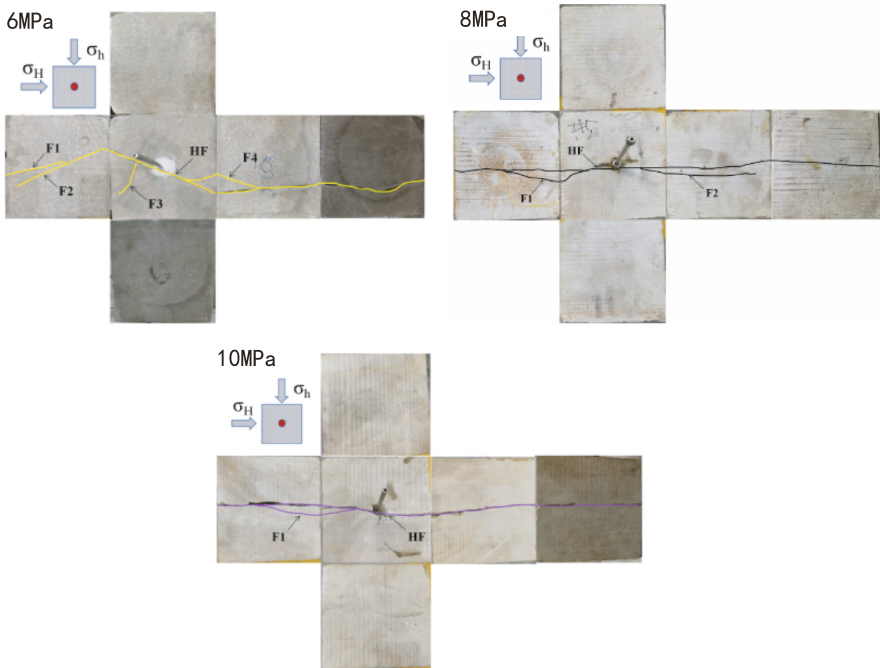


Fig. 9. Fracture morphology diagram formed by supercritical CO₂ fracturing under different stress differences

Based on the figure presented, when the horizontal stress difference is 6 MPa and the displacement is 30 mL/min, a hydraulic fracture with a direction of 26° to the maximum horizontal principal stress is generated after compression. During its expansion, the main fracture demonstrates a clear deviation, leading to the formation of two branch fractures with an included angle of 13°. Furthermore, branch fractures F3 and F4 are generated on both wings of the main fracture, inclined at angles of 86° and 34° with respect to the

main fracture, respectively. Upon increasing the horizontal stress difference to 8 MPa, hydraulic fractures HF propagate in the direction of the maximum horizontal principal stress, and branch fractures F1 and F2 appear at angles of 23° and 9°, respectively, with respect to the main fracture. Similarly, at a stress difference of 10 MPa, a hydraulic fracture HF extends along the direction of the maximum horizontal principal stress and triggers the formation of a branch fracture F1, inclined at an angle of 13° with the main fracture. Therefore, the smaller the horizontal stress difference, the more conducive it is to the multi-point initiation and turning of hydraulic fractures, thereby increasing the complexity of reservoir fractures and improving the effectiveness of oil and gas flow.

5 Conclusions

Supercritical CO₂ has the potential for reservoir transformation, carbon utilization, and carbon sequestration. Through the large-scale true triaxial fracturing experimental device, the impact of different fluids, displacement, and stress differences on the expansion of tight sandstone fractures is clarified. It is believed that under the guidance of the “dual carbon” goal, supercritical CO₂ fracturing technology has broad application prospects.

The fracture pressure of supercritical CO₂ fracturing is 13.9 MPa, which is 40.6% lower than that of slick water fracturing. The rock fracture time has increased by 274.1% compared to slick water fracturing. The fracture tortuosity formed by supercritical CO₂ fracturing is 2.23 times that of slick water fracturing. The spatial morphology of fractures formed by supercritical CO₂ is more complex, and the surface roughness is large.

In supercritical CO₂ fracturing, larger displacement and lower in-situ stress difference are more conducive to multi-branch initiation and fracture turning of hydraulic fractures, thereby increasing the complexity of the reservoir fractures and improving the flow capacity.

References

1. Yin, L.: Summary of experimental research on supercritical carbon dioxide fracturing technology. *China Mining Eng.* **50**(02), 45–47 (2021)
2. Zhang, J., Han, Z., Pan, J.: Overview of CO₂ anhydrous fracturing process and core equipment. *Petrol. Mach.* **44**(8), 79–84 (2016)
3. Li, S., Zheng, W.: Analysis of new CO₂ sealed sand mixing devices and liquid CO₂ fracturing cases abroad. *Drilling Prod. Technol.* (5) (2017)
4. Liu, B., Suzuki, A., Ito, T.: Numerical analysis of different fracturing mechanisms between supercritical CO₂ and water based fracturing fluids. *Int. J. Rock Mech. Mining Sci.* **132** (2020)
5. Xiaogang, L., Jialin, L., Jingyi, Z., et al.: Optimization of drag reducing agent system for supercritical carbon dioxide fracturing fluid. *Nat. Gas Ind.* **43**(04), 103–115 (2023)
6. Hou, B., Song, Z., Jia, J., et al.: Experimental study on the effect of supercritical carbon dioxide on the mechanical properties of tight sandstone. *China Offshore Oil Gas* **30**(005), 109–115 (2018)
7. Wang, M., Wang, H., Li, G., et al.: Numerical simulation of sand carrying in supercritical CO₂ fracturing fractures. *Petrol. Mach.* **046**(011), 72–78, 84 (2018)

8. Lu, J., Nicot, J.P., Mickler, P.J., et al.: Alteration of Bakken reserve rock during CO₂-based fracturing - an autoclave reaction experience. *J. Unconventional Oil Gas Resour.* **14**, 72–85 (2016)
9. Han, K.: Research and Application of Supercritical Carbon Dioxide Fracturing in Tight Sandstone Formation of Changqing XX Block. China University of Petroleum (Beijing) (2018)
10. Li, S.H., Zhang, S.C., Zou, Y.S., et al.: Experimental study on the impact of CO₂-brine-rock interaction on rock properties and fracture propagation during supercritical CO₂ fracturing in chang-7 tight sandstone formation. In: 53rd US Rock Mechanics/Geomechanics Symposium. OnePetro (2019)
11. Zhang, X., Lu, Y., Tang, J., et al.: Experimental study on fracture initiation and propagation in shale using supercritical carbon dioxide fracturing. *Fuel* **190**, 370–378 (2017)
12. Jiang, Y., Qin, C., Kang, Z., et al.: Experimental study of supercritical CO₂ fracturing on initiation pressure and fracture propagation in shale under different triaxial stress conditions. *J. Nat. Gas Sci. Eng.* **55**, 382–394 (2018)
13. Zhou, D., Zhang, G., Zhao, P., et al.: Effects of post-instability induced by supercritical CO₂ phase change on fracture dynamic propagation. *J. Petrol. Sci. Eng.* **162**, 358–366 (2018)
14. Zhou, D., Zhang, G., Prasad, M., et al.: The effects of temperature on supercritical CO₂ induced fracture: an experimental study. *Fuel* **247**, 126–134 (2019)
15. Chen, H., Hu, Y., Kang, Y., et al.: Fracture initiation and propagation under different perforation orientation angles in supercritical CO₂ fracturing. *J. Petrol. Sci. Eng.*, 106403 (2019)
16. Mian, C., Fei, P., Yan, J.: Simulation and analysis of large-scale true triaxial hydraulic fracturing. *J. Rock Mech. Eng.* **S1**, 868–872 (2000)
17. Liu, G., Pang, F., Chen, Z.: Similarity criteria in hydraulic fracturing simulation experiments. *J. Petrol. Univ. (Nat. Sci. Edn.)* (05), 45–48+6–5 (2000)
18. Feng, R., Memon, S., Giwelli, A., et al.: Supercritical CO₂ fracturing induced change in wellington shale: insights from laboratory. In: 54th US Rock Mechanics/Geomechanics Symposium OnePetro (2020)
19. Ye, L., Zou, Y., Zhao, Q., et al.: Experimental study on CO₂ fracturing fracture propagation in tight sandstone reservoirs. *Petrol. Drilling Prod. Technol.* **40**(03), 93–100 (2018)
20. Zhang, Y., Lou, Y., Mou, C., et al.: The effect of injection pressure on the mechanical characteristics of tight sandstone during supercritical carbon dioxide fracturing. *Petrol. Drilling Prod. Technol.* **041**(002), 242–248 (2019)